





Cite this: *RSC Adv.*, 2017, 7, 23392

# L-Ascorbyl 2,6-dipalmitate inhibits biofilm formation and virulence in methicillin-resistant *Staphylococcus aureus* and prevents triacylglyceride accumulation in *Caenorhabditis elegans*†

Sivasamy Sethupathy,  ‡ Loganathan Vigneshwari,  ‡ Alaguvel Valliammai,   
Krishnaswamy Balamurugan  and Shunmugiah Karutha Pandian \*

In the present study, the antibiofilm, antipathogenic and anticarotenogenic potential of L-ascorbyl 2,6-dipalmitate (ADP) against methicillin-resistant *Staphylococcus aureus* (MRSA) has been evaluated. ADP inhibited biofilm formation by MRSA in a concentration-dependent manner. Light and confocal laser scanning microscopic analyses further confirmed the potent antibiofilm activity of ADP. Furthermore, ADP treatment inhibited virulence factors without any influence on the growth/metabolic activity of MRSA. ADP treatment also affected the survival of MRSA in the presence of hydrogen peroxide, methylene blue and whole blood, and modulated the expression of genes involved in biofilm formation and virulence. The combination of ADP with antibiotics efficiently protects *Caenorhabditis elegans* from MRSA infection. Compounds that inhibit staphyloxanthin synthesis are known to inhibit triglyceride accumulation in eukaryotes. Hence in the current study, the anti-obesity potential of ADP was also evaluated using the model nematode *C. elegans*. The results revealed the ability of ADP to mitigate triacylglyceride accumulation without affecting food consumption or reproduction. FTIR analysis also confirmed the reduction of fat accumulation. qPCR analysis revealed the ability of ADP to interfere with the expression of genes involved in fatty acid synthesis and insulin signalling. In addition, molecular docking analysis predicted the ability of ADP to interact with proteins involved in staphyloxanthin and oleic acid biosynthesis and stearoyl-coenzyme A desaturase-1 in MRSA, *C. elegans* and humans, respectively. The results obtained in the present study suggest that ADP could be utilized as a potent antipathogenic and anti-obesity agent.

Received 10th March 2017  
Accepted 11th April 2017

DOI: 10.1039/c7ra02934a

rsc.li/rsc-advances

## 1. Introduction

Biofilm formation by bacterial pathogens on/within indwelling medical devices and implants poses a serious threat in clinical settings.<sup>1</sup> According to reports by the Centre for Disease Control<sup>2</sup> (CDC) and National Institute of Health<sup>3</sup> (NIH), 65 to 80% of bacterial infections are associated with biofilm formation. Biofilms are a monospecies/multi-species microbial assemblage encased in self-secreted extracellular polymeric substances (EPS; including proteins, polysaccharides and extracellular DNA) formed on biotic and abiotic surfaces.<sup>4</sup> Most bacterial pathogens have an innate ability to form a highly

protective biofilm to escape from host immune responses and antimicrobial agents.<sup>5</sup> Formation of a biofilm provides multi-level protection to microbes against antibiotics, due to the slower growth rate and altered metabolism of microbes in biofilms, the production of dormant persister cells, and EPS-mediated blockage of the penetration of antimicrobial agents.<sup>6</sup> When compared to planktonic cells, bacterial cells that reside in a biofilm matrix are highly resistant to antibiotics.<sup>7</sup> Hence, biofilm formation by bacterial pathogens has been considered as a major cause of therapeutic failure and antimicrobial resistance development.<sup>8</sup>

*Staphylococcus aureus* is a versatile bacterium present in 30% of the human population as a commensal bacterial species,<sup>9</sup> and it has been recognized as a leading cause of healthcare-associated infections (HAIs), device-related infections (DVIIs) and community-acquired infections (CAIs).<sup>10</sup> In recent years, *S. aureus* has gained greater public attention owing to its mortality and the emergence of resistance against vancomycin and methicillin.<sup>11</sup> *S. aureus* utilizes biofilm formation as one

Department of Biotechnology, Alagappa University, Science Campus, Karaikudi 630 003, Tamil Nadu, India. E-mail: sk\_pandian@rediffmail.com; Fax: +91 4565 225202; Tel: +91 4565 225215

† Electronic supplementary information (ESI) available. See DOI: 10.1039/c7ra02934a

‡ These authors contributed equally to this work.



pathogenic mechanism to cause mild to severe nosocomial and medical device-associated infections.<sup>12</sup> Biofilm formation in *S. aureus* involves the following steps: initial adherence of the cells to a solid substratum, an increase in biomass, EPS secretion, microcolony formation, biofilm maturation and dispersion.<sup>13</sup> Biofilm formation by *S. aureus* in wounds, catheters and prosthetic joints with an elevated level of antibiotic tolerance/resistance to antibiotics has led to a bottleneck situation in clinical settings.<sup>14</sup> Hence, biofilm formation has been considered as an Achilles' heel to inhibiting the clinical manifestation of *S. aureus*.<sup>15</sup>

In addition to biofilm formation, *S. aureus* is known to produce an array of cell bound/surface virulence factors [coagulase, protein A, elastin-binding protein, collagen binding protein, fibronectin binding protein and clumping factor] and exotoxins/virulence enzymes [ $\alpha$ -hemolysin,  $\beta$ -hemolysin,  $\gamma$ -hemolysin, leukocidin, and panton-valentine leukocidin (PVL), staphylococcal enterotoxins (SEA, SEB, SEcN, SED, SEE, SEG, SEH, and SEI), exfoliative toxins (ETA and ETB), toxic shock syndrome toxin-1, nucleases, proteases, lipases, hyaluronidase, and collagenase] to outwit the robust innate and adaptive immune responses.<sup>16</sup> Furthermore, *S. aureus* produces a golden orange-red triterpenoid carotenoid pigment called staphyloxanthin, which has antioxidant activity and protects against  $H_2O_2$ ,  $OH^*$  and neutrophil-mediated killing, hence promoting virulence.<sup>17</sup> Biosynthesis of staphyloxanthin requires five enzymatic reaction processes: (1) synthesis of dehydrosqualene through condensation of  $2 \times$  farnesyl diphosphate by dehydrosqualene synthase CrtM; (2) dehydrosqualene desaturase CrtN-driven oxidation of dehydrosqualene to 4,4'-diaponeurosporene; (3) synthesis of 4,4'-diaponeurosporenic acid through oxidation of the terminal methyl group of 4,4'-diaponeurosporene by diaponeurosporene oxidase CrtP; (4) formation of glycosyl-4,4'-diaponeurosporenoate by glycosyltransferase CrtQ-mediated esterification of glucose at the C1' position with a carboxyl group of 4,4'-diaponeurosporenic acid; and (5) finally, acyltransferase CrtO-mediated staphyloxanthin synthesis by esterification of glucose at the C6' position with the carboxyl group of 12-methyltetradecanoic acid.<sup>18</sup>

Methanolic extracts of marine alga *Padina boergeresii* and the corresponding L-ascorbyl 2,6-dipalmitate (ADP)-rich fractions have been previously reported to have the ability to inhibit biofilm formation by MRSA.<sup>19</sup> ADP is a fatty ester derivative of ascorbic acid and it has been used as an antioxidant and skin whitening agent in cosmetic preparations.<sup>20</sup> In addition, based on a safety evaluation, a Cosmetic Ingredient Review (CIR) expert panel has confirmed that ADP is a generally regarded as safe (GRAS) ingredient.<sup>21</sup> Feeding F344 rats an ADP-supplemented (5%) diet for 32 weeks does not have any negative impact.<sup>22</sup> Hence the possibility of ADP toxicity has been ruled out. The effect of ADP treatment on biofilm formation by MRSA was assessed in the current investigation using standard qualitative and quantitative assays. Furthermore, the action of ADP on virulence factors such as slime, lipase, autolysin, and hemolysin was also examined. In addition, the effects of co-treatment/combination of ADP with certain antibiotics on the growth of MRSA were also analysed. Cholesterol-lowering drugs

have been shown to inhibit staphyloxanthin pigment production by *S. aureus*.<sup>23</sup> The nematode *Caenorhabditis elegans* is recognised as a model system to study fat synthesis, storage and metabolism.<sup>24</sup> Comparative genomic and functional analysis of the genes involved in lipid metabolism in *C. elegans* revealed that 70% of the genes have human orthologs.<sup>25</sup> Hence, *C. elegans* has been successfully used as an *in vivo* model for screening anti-obesity/lipid-lowering drugs.<sup>26</sup> ADP exhibited potent inhibitory activity against staphyloxanthin production by MRSA, and hence the present study was further extended to evaluate the anti-obesity potential of ADP through analysing the effect of ADP on triacylglyceride accumulation in *C. elegans* fed with a high fat diet (*i.e.* standard nematode growth medium (NGM) supplemented with 25  $\mu$ M cholesterol).

## 2. Materials and methods

### 2.1. Ethics statement

Healthy human blood and plasma were used in the present study to analyse the effect of ADP treatment on the hemolysin production, blood survival and biofilm formation of *Staphylococcus aureus* MRSA [ATCC 33591]. The experimental procedures and the use of healthy human blood was evaluated and approved by the Institutional Ethical Committee, Alagappa University, Karaikudi (IEC Ref No: IEC/AU/2016/1/4). The blood samples from healthy individuals were collected by trained personnel as per the standard guidelines and "written informed consent" was obtained from all subjects. All experiments were performed in compliance with the relevant laws and institutional guidelines (Ethical Guidelines for Biomedical Research on Human Participants, Indian Council of Medical Research, India).

### 2.2. Bacterial strains and culture conditions

*Staphylococcus aureus* MRSA [ATCC 33591] was grown and maintained on tryptic soy agar/broth (TSA/TSB) at 37 °C and stored at 4 °C. For biofilm formation, TSB containing 0.25% glucose (TSBG) was used. *Escherichia coli* OP50, used as a *Caenorhabditis elegans* food source, was obtained from CGC and maintained on LB agar/broth at 37 °C and stored at 4 °C.

### 2.3. Antibiofilm assay, and light and confocal laser scanning microscopic observation of biofilms

ADP (CAS No: 4218-81-9) was procured from TCI Chemicals (India) Pvt. Ltd and dissolved in acetone to form a 10 mg mL<sup>-1</sup> stock. The antibiofilm activity of ADP was assessed using a 24-well micro titre plate (MTP) assay.<sup>27</sup> Briefly, each well containing 1 mL of TSBG was inoculated with an overnight culture of MRSA to an initial optical density (OD) of 0.05 at 600 nm, supplemented with 10 to 100  $\mu$ g mL<sup>-1</sup> of ADP with the concentration increasing in 10  $\mu$ g mL<sup>-1</sup> increments, and incubated for 24 h at 37 °C. After incubation, the growth of MRSA was measured at 600 nm. For biofilm quantification, cells adhered on the wells were stained with 0.4% crystal violet (CV) staining solution (w/v) for 5 min. Then, the CV-stained biofilms were destained using 10% glacial acetic acid for 10 min, and the optical density was



measured at 570 nm using a multi-label reader (Spectramax M3, USA). In addition, the effect of ADP treatment on the initial attachment<sup>28</sup> and biofilm formation of MRSA on plasma-coated surfaces was also analysed.<sup>29</sup> Biofilms formed in the presence and absence of ADP were visualised under light and confocal laser scanning microscopes.<sup>30</sup> Detailed procedures are presented in the ESI.†

#### 2.4. Ring biofilm inhibition assay

The effect of ADP on ring biofilm formation at the air–liquid interface was assessed by growing MRSA in glass tubes containing 2 mL of TSB supplemented with or without 20 to 100  $\mu\text{g mL}^{-1}$  of ADP (with the concentration of ADP increasing in 20  $\mu\text{g mL}^{-1}$  increments) for 48 h at 37 °C with shaking at 160 rpm. After incubation, the tubes were visually observed and photographed.

#### 2.5. Effect of ADP on autoaggregation, slime production, colony morphology and virulence factor production of MRSA

Autoaggregation of control and ADP-treated MRSA cells was assessed spectrometrically.<sup>31</sup> The effect of ADP on slime synthesis<sup>32</sup> and colony morphology was assessed on Congo red agar and tryptic soy agar, respectively, and the agars were visually observed and photographed. Cell-free culture supernatant (CFCS) from MRSA grown in the presence or absence of 10 to 100  $\mu\text{g mL}^{-1}$  of ADP (with the concentration of ADP increasing in 10  $\mu\text{g mL}^{-1}$  increments) was collected by centrifugation and used for hemolysin<sup>33</sup> and lipase assays.<sup>34</sup> The cell pellets were used for analysis of autolysin production,<sup>35</sup> and extraction and quantification of staphyloxanthin pigment.<sup>36</sup> Detailed procedures are presented in the ESI.†

#### 2.6. Effect of ADP on staphyloxanthin inhibition and survival of MRSA in whole blood, and in the presence of $\text{H}_2\text{O}_2$ and singlet oxygen (methylene blue)

MRSA control and ADP-treated cells were incubated in freshly drawn blood (heparinized),<sup>36</sup> PBS containing 1 mM hydrogen peroxide ( $\text{H}_2\text{O}_2$ )<sup>36</sup> and 10  $\mu\text{g mL}^{-1}$  of methylene blue,<sup>36</sup> and the number of viable cells was determined. Detailed procedures are presented in the ESI.†

#### 2.7. Growth curve and 2,3-bis-(2-methoxy-4-nitro-5-sulfophenyl)-2H-tetrazolium-5-carboxanilide (XTT) assay

To analyse the effect of the biofilm inhibitory concentration of ADP (100  $\mu\text{g mL}^{-1}$ ) on the growth of MRSA, the optical density was measured at 600 nm over a period of 24 h at 1 h intervals. In addition, the metabolic activity and viability of MRSA grown in the absence and presence of ADP (100  $\mu\text{g mL}^{-1}$ ) were assessed using an XTT assay.

#### 2.8. *C. elegans* maintenance and toxicity assay

Wild-type N2 Bristol *C. elegans* was obtained from the Caenorhabditis Genetics Center and maintained in nematode growth medium (NGM).<sup>37</sup> To study the effect of ADP on fat accumulation, wild-type N2 Bristol *C. elegans* was raised in NGM

containing a normal diet (12.5  $\mu\text{M}$  cholesterol), a high fat diet (25  $\mu\text{M}$  cholesterol) and a high fat diet supplemented with 100 or 200  $\mu\text{g mL}^{-1}$  of ADP with an *E. coli* OP50 lawn. The animals were age-synchronized by bleaching with commercial bleach with 5 M KOH. Age-synchronized young adult animals were used for various physiological assays and gene expression studies.

To evaluate the toxicity of ADP, age-synchronized L4 stage animals ( $N = 20$ ) were transferred to NGM plates supplemented with 0 (control), 200, 400, 800 or 1600  $\mu\text{g mL}^{-1}$  of ADP. In addition, 40  $\mu\text{M}$  5-fluorodesoxyuridine (FUDR) was added to the NGM plates to prevent the hatching of eggs. The worms were observed under an inverted microscope and the number of viable worms was counted every 24 h. The animals were considered to be dead when they did not respond to gentle tapping or touching with a platinum worm picker loop.<sup>38</sup>

#### 2.9. Determination of minimum inhibitory concentrations of antibiotics and evaluation of a combination of ADP and antibiotics on the growth of MRSA

The MICs of oxacillin (OXI), linezolid (LNZ), vancomycin (VAN) and rifampicin (RIF) were determined using the broth micro-dilution method as per the instructions provided by the Clinical and Laboratory Standards Institute. To investigate the ability of ADP to enhance the activity of antibiotics, MRSA was grown in the presence or absence of 100  $\mu\text{g mL}^{-1}$  of ADP and sub-MICs of OXI, LNZ, VAN and RIF for 24 h. After incubation, the cell density was measured spectrometrically at 600 nm.

#### 2.10. Effect of a combination of ADP and antibiotics on the survival of *C. elegans* upon MRSA infection

To evaluate the combination of ADP and antibiotics on the survival of *C. elegans* upon MRSA infection, age-synchronized L4 stage animals ( $N = 20$ ) were transferred to a 24-well plate containing 1 mL of sterile M9 buffer supplemented with or without 100  $\mu\text{g mL}^{-1}$  of ADP, 0.01  $\mu\text{g mL}^{-1}$  of rifampicin or a combination of 100  $\mu\text{g mL}^{-1}$  ADP + 0.01  $\mu\text{g mL}^{-1}$  rifampicin. A three-hour culture of MRSA was added (20% inoculum) to each well, and the plates were incubated at 20 °C and examined for the survival of *C. elegans*. The worms were observed under an inverted microscope and the number of viable worms was counted every 24 h. The animals were considered to be dead if they did not respond to gentle tapping or touching with a platinum worm picker loop. *C. elegans* fed with *E. coli* OP50 (a laboratory food source) served as a control.

#### 2.11. Quantitative real-time PCR analysis

Total RNA was extracted from control and 100  $\mu\text{g mL}^{-1}$  ADP-treated MRSA using the Trizol method and converted into cDNA using a Superscript III kit (Invitrogen Inc., USA). Quantitative real-time PCR analysis (qPCR) was performed on an Applied Biosystems thermal cycler using the Power SYBR Green PCR Master Mix. The Ct value of *gyrB* (gyrase) in each sample was calculated using a relative relationship method supplied by the manufacturer (Applied Biosystems). Details of the qPCR thermal conditions and the primer sequences of the genes



(*agrA*, *agrC*, *sarA*, *sigB*, *saeS*, *icaA*, *icaD*, *fmbA*, *fmbB*, *clfA*, *cna*, *epbs*, *altA*, *sea*, *sspB*, *aur*, *hld*, *hla*, *geh* and *crtM*) used in this study are given as ESI.†

## 2.12. Estimation of triglycerides

Control, high fat diet-fed and high fat diet supplemented with 100 or 200  $\mu\text{g mL}^{-1}$  ADP-fed *C. elegans* were washed with M9 buffer and sonicated in triglyceride assay buffer. After sonication, the *C. elegans* lysates were centrifuged at 10 000 rpm for 10 min to collect the supernatants. The triacylglyceride content was measured using a BioVision triglyceride assay kit (Mountain view, CA, USA) as per the manufacturer's protocols. In addition, the protein content was also quantified using a Bradford assay kit (BioRad).

## 2.13. Visualization of *C. elegans* stained with Oil Red and Sudan Black under a bright field microscope

Age-synchronized L4 stage worms were washed twice with phosphate-buffered saline (PBS, pH 7.4) and fixed in PBS containing 1% paraformaldehyde for 1 h at 4 °C. After fixation, the paraformaldehyde-fixed worms were subjected to 2 freeze-thaw cycles and washed twice with PBS to remove residual paraformaldehyde. Then, the worms were dehydrated with 60% isopropanol for 15 min at room temperature. After incubation, the 60% isopropanol was pipetted out and the worms were stained with Oil Red O (6 volumes of 5 mg  $\text{mL}^{-1}$  Oil Red O in isopropanol and 4 volumes of MilliQ water) for 6 h.<sup>39</sup> For Sudan Black staining, the worms were washed and fixed as mentioned previously. Dehydration was done using 60% ethanol for 15 min at room temperature and the worms were stained with Sudan Black staining solution (6 volumes of 1 mg  $\text{mL}^{-1}$  Sudan Black in ethanol and 4 volumes of ethanol) for 12 h. After staining, the worms were washed with PBS and observed under a light microscope.<sup>39</sup>

## 2.14. FTIR analysis

An equal number ( $N = 50$ ) of control, high fat diet-fed and high fat diet supplemented with 100 or 200  $\mu\text{g mL}^{-1}$  of ADP-fed *C. elegans* were ground with 150 mg of potassium bromide and dried under vacuum to prepare a pellet. Infrared spectra were then collected in the range of 400 to 4000  $\text{cm}^{-1}$  using an FTIR spectrometer (Bruker Tensor 27) and the values were plotted as intensity against wavenumber.<sup>40</sup>

## 2.15. Pharyngeal pumping assay

To determine the pumping rate of the pharynx, control, high fat diet-fed and high fat diet supplemented with 100 or 200  $\mu\text{g mL}^{-1}$  of ADP-fed *C. elegans* were placed on separate NGM plates seeded with OP50. Pharyngeal pumping was observed carefully for 10 s under a stereomicroscope.<sup>41</sup>

## 2.16. Food consumption assay

The effect of ADP treatment on food consumption was evaluated by incubating *C. elegans* in M9 buffer containing UV-killed *E. coli* OP50 (OD 600 = 0.4) for 36 h at 20 °C, and the OD of the

M9 buffer was measured at different time intervals. A reduction in cell density was considered as active food consumption.<sup>42</sup>

## 2.17. Egg laying assay

Age-synchronized young adult worms were transferred to standard NGM containing *E. coli* OP50 lawns. The number of eggs laid and progenies produced by individual worms was counted for 6 days.<sup>40</sup>

## 2.18. Locomotion assay

The locomotion of control, high fat diet-fed and high fat diet supplemented with 100 or 200  $\mu\text{g mL}^{-1}$  of ADP-fed *C. elegans* was quantified by counting the number of forward body bends per min under an inverted light microscope at 8× magnification.<sup>43</sup>

## 2.19. Reactive oxygen species (ROS) assay

Control, high fat diet-fed and high fat diet supplemented with 100 or 200  $\mu\text{g mL}^{-1}$  of ADP-fed *C. elegans* were washed thoroughly with M9 buffer to remove any adhered bacterial cells. Approximately 40–50 worms were incubated with 5  $\mu\text{g mL}^{-1}$  of 2',7'-dichlorodihydro-fluorescein diacetate ( $\text{H}_2\text{DCFDA}$ ) for 30 min at 20 °C in the dark. After incubation, 30 mM sodium azide ( $\text{NaN}_3$ ) were used to anesthetize the worms and the worms were visualised under a fluorescence microscope (Nikon Eclipse Ti-S, Japan).<sup>44</sup>

## 2.20. Quantitative real-time PCR analysis

Total RNA was extracted from control, high fat diet-fed and high fat diet supplemented with 200  $\mu\text{g mL}^{-1}$  of ADP-fed *C. elegans* using the Trizol method and converted into cDNA using a Superscript III kit (Invitrogen Inc., USA). Quantitative real-time PCR analysis (qPCR) was performed on an Applied Biosystems thermal cycler using the Power SYBR Green PCR Master Mix. The Ct value of the  $\beta$ -actin in each sample was calculated using a relative relationship method supplied by the manufacturer (Applied Biosystems). Details of the qPCR thermal conditions and the primer sequences of the genes (*atgl-1*, *daf-2*, *daf-16*, *ins-7*, *sod*, *eat-2*, *skn-1*, *aak-1*, *akt-1*, *age-1*, *egl-8*, *sams-1*, *fat-5*, *sgk-1* and *acs-1*) used in this study are given as ESI.†

## 2.21. Molecular docking analysis

The crystal structures of dehydroxysqualene synthase CrtM (ID: 2ZCO) and stearoyl-coenzyme A desaturase-1 (ID: 4ZYO) were retrieved from the protein data bank. The modelled structures of delta(9)-fatty-acid desaturases such as fat-5 (ID: FAT6\_CAEEL), fat-6 (ID: FAT6\_CAEEL) and fat-7 (ID: FAT6\_CAEEL) were downloaded from the protein model portal and the chemical structure of ADP was downloaded from PubChem (CID: 54722209). Molecular docking was carried out using Glide version 5.5 (Schrödinger Inc., New York, USA).<sup>45</sup>

## 2.22. Statistical analysis

All the experiments were performed independently in triplicate. Data were analyzed by one-way analysis of variance (ANOVA),





with a significance  $p$ -value of 0.05, using the SPSS (Chicago, IL, USA) statistical software package.

### 3. Results and discussion

#### 3.1. Effect of ADP on initial attachment, biofilm formation, autoaggregation, virulence factor production, blood survival and growth of MRSA

Biofilm formation has been identified as an indispensable virulence mechanism of *S. aureus* responsible for its pathophysiology, antibiotic resistance and survival under *in vivo* conditions.<sup>1</sup> MRSA biofilms formed on indwelling medical devices are difficult to treat/remove.<sup>46</sup> Hence, inhibition of biofilm formation has become an alternative therapeutic strategy to control infections caused by MRSA. Bioactive compounds with the ability to inhibit biofilm formation and other virulence factors, such as hemolysin, lipase, autolysin, staphyloxanthin and hyaluronidase, could be useful in controlling infections caused by MRSA.

The ability of standard ADP to inhibit biofilm formation by MRSA was assessed using a standard 24-well MTP assay coupled with CV staining (Fig. 1a) and spectrophotometric quantification. The results revealed concentration-dependent inhibition of MRSA biofilm formation. Notably, 50 and 90% biofilm inhibition was observed at 50 and 100  $\mu\text{g mL}^{-1}$  of ADP and these concentrations were denoted as the sub-BIC and BIC, respectively (Fig. 1b). The biofilm inhibition observed in the present study falls in line with the antibiofilm activity shown by red wines<sup>47</sup> and coral-associated bacterial extracts<sup>29</sup> in terms of percentage of biofilm reduction. In addition, ADP also exhibited dose-dependent inhibition of the initial adherence of MRSA to plastic surfaces (Fig. 1b). A plasma coating on glass and plastic surfaces mimics the *in vivo* conditions and allows MRSA to form a robust biofilm.<sup>29</sup> Hence, the ability of ADP to inhibit biofilm formation on plasma-coated glass and polystyrene surfaces has been analysed. Spectrophotometric quantification revealed the ability of ADP to inhibit MRSA biofilm formation on the plasma-coated polystyrene surface (Fig. 1b). The antibiofilm activity of ADP was further confirmed using light microscope and CLSM analysis. The light micrographs showed the reduction of biofilm formation on both glass and plasma-coated glass surfaces (Fig. 1c). CLSM analysis clearly showed a typical multi-layer of adherent cells with microcolony and macrocolony formation in the MRSA control. In contrast, the MRSA biofilm formed in the presence of 50 and 100  $\mu\text{g mL}^{-1}$  of ADP showed reduced formation of a multi-layer of adherent cells, as well as reduced surface colonization and thickness (Fig. 1d). These results further confirm the potent antibiofilm activity of ADP against MRSA. Similar to Gram-negative bacteria, MRSA also forms a ring biofilm at the air-liquid interface. The results of the ring biofilm assay clearly show the ability of ADP to inhibit biofilm formation at the air-liquid interface (Fig. 1e). Autoaggregation has been reported as an important event in biofilm formation.<sup>48</sup> Interestingly, addition of ADP to the growth medium reduced the autoaggregation of MRSA in a concentration-dependent manner (Fig. 1f). The non-toxic nature of ADP and its ability

to inhibit biofilm formation and autoaggregation of MRSA is of great significance for drug development.

AIP-mediated signalling is present in a wide range of Gram-positive pathogens.<sup>49</sup> Therefore, we have evaluated the effect of ADP on biofilm formation by *Staphylococcus epidermidis* and *Enterococcus faecalis*. In addition, the antibiofilm activity of ADP was evaluated against Gram-negative and Gram-positive pathogens such as *Pseudomonas aeruginosa*, *Serratia marcescens*, *Vibrio harveyi*, *Vibrio parahaemolyticus*, *Vibrio alginolyticus*, *Escherichia coli*, *Proteus mirabilis*, *Proteus vulgaris*, *Klebsiella pneumoniae*, *Streptococcus mutans* and *Bacillus subtilis*. The results revealed the absence of antibiofilm activity at 1  $\text{mg mL}^{-1}$  of ADP (Fig. 2). Hence, we assume that the antibiofilm activity of ADP against MRSA could be due to the modulation of specific mechanism(s).

Biofilm inhibitors have been reported to inhibit slime synthesis in *S. aureus*.<sup>29,50,51</sup> Hence in the present study, the effect of ADP on slime production was assessed using a CRA plate assay. The results showed a reduction in the Bordeaux red colouration of the colonies and black colouration around them (Fig. 3a). These results suggested that ADP was able to interfere with EPS production. A recent report stated that the reduction of slime synthesis by berberine is attributed to the inhibition of amyloid fibril formation of MRSA.<sup>50</sup> In addition, colonies of MRSA on TSB agar without ADP were found to be smooth and mucoid, and exhibit a spreading pattern, whereas in the presence of ADP (100  $\mu\text{g mL}^{-1}$ ) on TSB agar, MRSA formed rough and non-spreading colonies (Fig. 3b).

Autoaggregation and biofilm formation of *S. aureus* requires autolysin-mediated eDNA release. Autolysin (*AtlA*) mutants have been reported to be defective in biofilm formation<sup>48</sup> and hence the effect of ADP treatment on autolysin production in MRSA was assessed spectrophotometrically. The results showed the presence of active lysis in the control cells, whereas in the ADP-treated cells, a dose-dependent reduction in autolysis was observed in the presence of 0.02% Triton X-100 (Fig. 3c). These results suggest that inhibition of autoaggregation and autolysin production by ADP could be one of the mechanisms responsible for the impairment of biofilm formation.

Furthermore, the effect of ADP on lipase and protease production was also analysed. Lipase produced by *S. aureus* is responsible for accumulation of granulocytes and protects the cells from antimicrobial lipids secreted by the human skin. The results of the lipase assay showed that ADP was able to inhibit lipase production in a concentration-dependent manner (Fig. 3d). In addition to biofilm formation, *S. aureus* depends on an array of cytotoxins that assault the innate immune cells, and these cytotoxins have been shown to have a pivotal role in establishing infections under *in vivo* conditions.  $\alpha$ -Hemolysin is one such important virulence factor produced by *S. aureus* involved in the necrosis of host cells that forms a  $\beta$ -barrel transmembrane aqueous channel with a diameter of 14 Å to allow the transport of  $\text{K}^+$  and  $\text{Ca}^{2+}$  ions. Importantly, lymphocytes and monocytes are highly susceptible to  $\alpha$ -hemolysin.<sup>52</sup> Hence, inhibition of hemolysin production in *S. aureus* is a plausible strategy to mitigate cellular damage during infection. The results of the hemolysin assay revealed a concentration-dependent



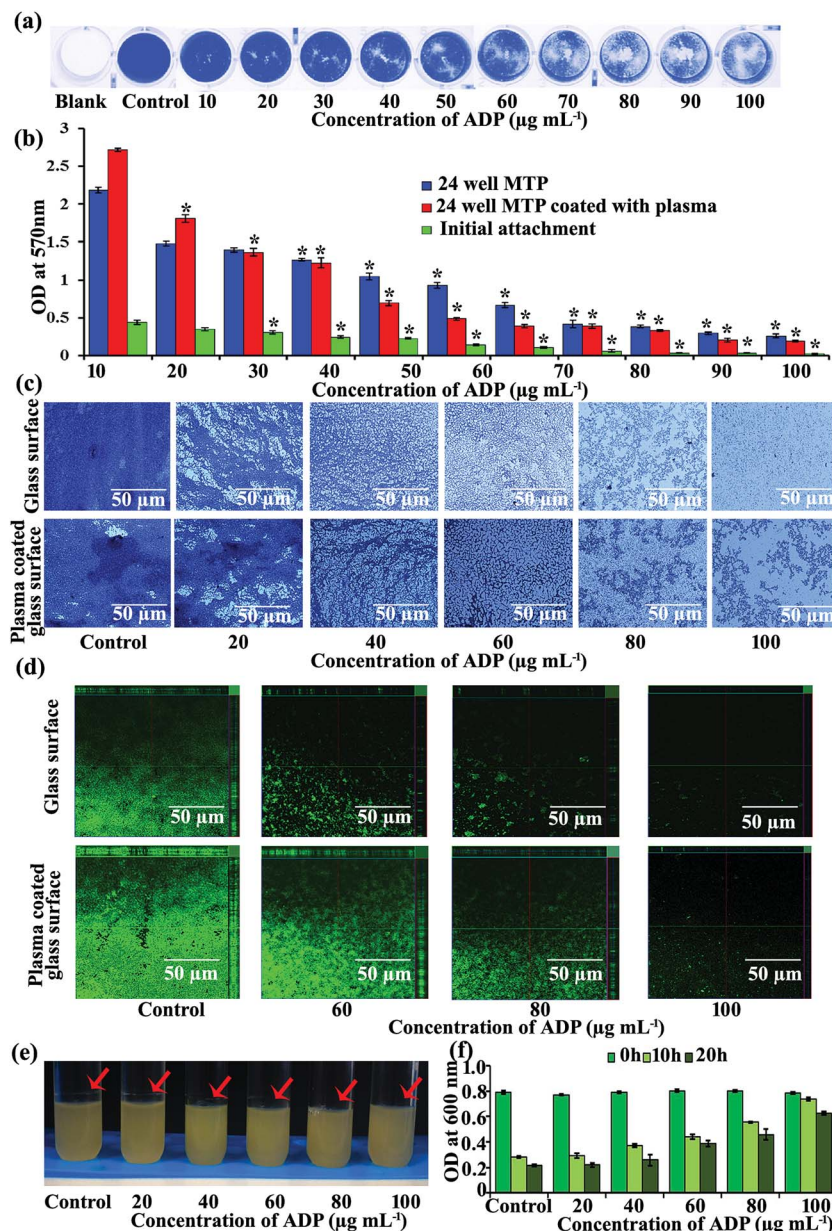


**Fig. 1** Antibiofilm activity of ADP against MRSA. 24-well MTP plate depicting concentration-dependent inhibition of MRSA biofilm formation (a). Effect of ADP treatment on biofilm formation on polystyrene and plasma-coated surfaces, and the initial attachment of MRSA (b). Light (c) and confocal laser scanning microscopic (d) observation of MRSA biofilms formed on glass and plasma-coated surfaces in the presence and absence of ADP. ADP inhibits the ring biofilm formation of MRSA at the air liquid interface (e). Effect of different concentrations of ADP on the autoaggregation of MRSA (f). Error bars indicate SDs from the mean ( $n = 6$  (biological triplicates in technical duplicates)). Asterisks indicate a statistically significant difference ( $p < 0.05$ ).

reduction in hemolysin production upon ADP treatment. Briefly, 50% and complete inhibition of hemolysin was observed at 30 and 70  $\mu\text{g mL}^{-1}$  of ADP (Fig. 3d). Hemolysin production is also related to biofilm formation in *S. aureus* and hence the biofilm inhibition by ADP may be attributed to its hemolysin inhibitory activity. Compounds like 1,3-benzodioxoles and benzo-1,4-dioxanes are found to inhibit autoinducing peptide (AIP)-regulated lipase and  $\alpha$ -hemolysin production in *S. aureus*.<sup>53</sup> Inhibition of lipase and hemolysin production by ADP suggests that it is able to interfere with AIP-mediated signalling in *S. aureus*.

*S. aureus* depends on the antioxidant potential of a carotenoid pigment called staphyloxanthin for its survival under adverse *in vivo* conditions and to escape from innate immune responses.<sup>37</sup> Inhibition of staphyloxanthin has been reported to increase neutrophil-mediated killing and affect the survival of *S. aureus* in the presence of oxidants.<sup>35</sup> Hence, the inhibition of staphyloxanthin pigment production is one of the therapeutic strategies to make *S. aureus* more susceptible to antibiotics and immune responses. Benzofuran derivatives, the cholesterol biosynthesis inhibitor phosphonosulfonate BPH-652 (ref. 23) and the human squalene synthase inhibitor zaragozic acid<sup>54</sup>



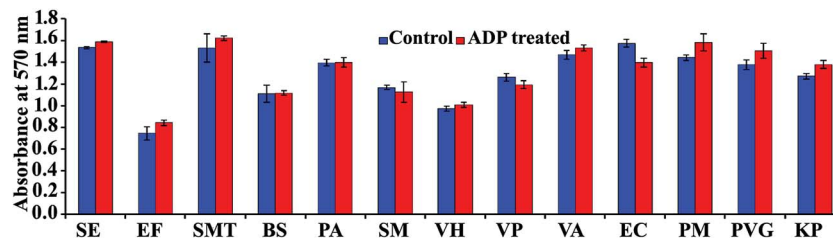


Fig. 2 Effect of ADP treatment ( $1 \text{ mg mL}^{-1}$ ) on the biofilm formation of *S. epidermidis* (SE), *E. faecalis* (EF), *S. mutans* (SMT), *B. subtilis* (BS), *P. aeruginosa* (PA), *S. marcescens* (SM), *V. harveyi* (VH), *V. parahaemolyticus* (VP), *V. alginolyticus* (VA), *E. coli* (EC), *P. mirabilis* (PM), *P. vulgaris* (PVG) and *K. pneumoniae* (KP). Error bars indicate SDs from the mean ( $n = 6$  (biological triplicates in technical duplicates)).

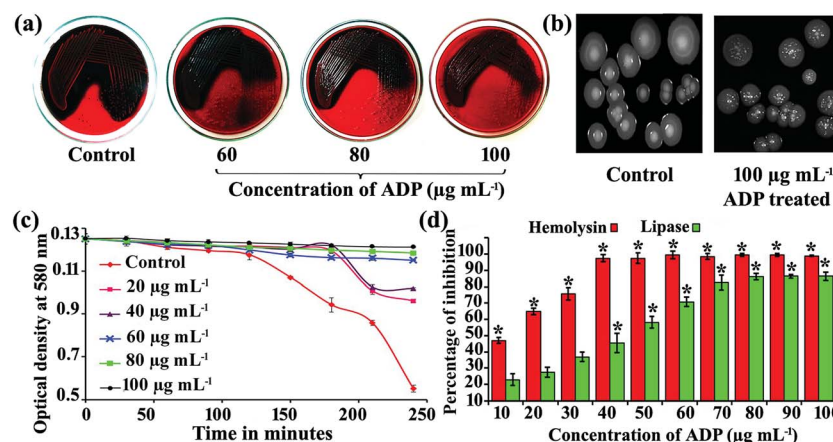


Fig. 3 Antipathogenic potential of ADP against MRSA. Effect of ADP treatment on slime synthesis of MRSA. Inhibition of the Bordeaux red coloration of the colonies indicates the slime inhibitory potential of ADP (a). Photographs depicting the effect of  $100 \text{ µg mL}^{-1}$  of ADP on the colony morphology of MRSA (b). ADP inhibits the production of autolysin (c), hemolysin and lipase (d) in a concentration-dependent manner. Error bars indicate SDs from the mean ( $n = 6$  (biological triplicates in technical duplicates)). Asterisks indicate a statistically significant difference ( $p < 0.05$ ).

have been reported to have strong inhibitory activity against staphyloxanthin production in MRSA. ADP inhibited staphyloxanthin production in a concentration-dependent manner (Fig. 4a and b). In addition, the effect of ADP on staphyloxanthin production in MRSA was also assessed by measuring the amount of staphyloxanthin and its metabolic intermediates, including 4,4'-diapophytoene, 4,4'-diaponeurosporene and 4,4'-diaponeurosporenic acid, spectrophotometrically. The results revealed the concentration-dependent inhibitory activity of ADP against 4,4'-diapophytoene (Fig. 4c), 4'-diaponeurosporene (Fig. 4d), 4'-diaponeurosporenic acid (Fig. 4e) and staphyloxanthin (Fig. 4f) production in MRSA.

Since staphyloxanthin protects MRSA from oxidative stress and the host innate immune responses,<sup>35</sup> we also assessed the effect of ADP treatment on the survival of MRSA in whole blood, and the sensitivity of MRSA to  $\text{H}_2\text{O}_2$  and methylene blue. The results showed that the survival of MRSA control cells in whole blood did not change. In contrast, the ADP-treated MRSA cells were highly sensitive to whole blood (Fig. 4g). As expected, the ADP-treated MRSA cells were highly susceptible to  $\text{H}_2\text{O}_2$  (Fig. 4h) and methylene blue (Fig. 4i) in comparison to control cells. These results further confirmed the potential of ADP to inhibit staphyloxanthin pigment production and consequently

the survival of MRSA in the presence of oxidants and neutrophils. The results observed in the present study correlate well with a previous report, in which rhodomymrtone was found to affect staphyloxanthin biosynthesis, the survival of MRSA in whole blood and the susceptibility of MRSA towards  $\text{H}_2\text{O}_2$  and methylene blue.<sup>35</sup>

An ideal antibiofilm/antipathogenic agent is expected to not have any negative influence on the proliferation and basic metabolic activity of the pathogens.<sup>36</sup> Growth curve analysis was performed to study the effect of ADP ( $100 \text{ µg mL}^{-1}$ ) on the growth of MRSA and the kinetic growth measurements suggested that ADP was non-bactericidal/bacteriostatic in nature (Fig. 4j). In addition, an XTT assay also showed an insignificant difference in the metabolic activity of control MRSA and MRSA treated with different concentrations of ADP (Fig. 4k).

### 3.2. Effect of a combination of ADP and antibiotics on the growth of MRSA

To evaluate the non-toxic nature of ADP, age-synchronized *C. elegans* N2 worms were treated with 200 to  $1600 \text{ µg mL}^{-1}$  of ADP throughout their lifespan. The toxicity of ADP was ruled out, as  $800 \text{ µg mL}^{-1}$  of ADP did not alter the lifespan of the *C. elegans* N2





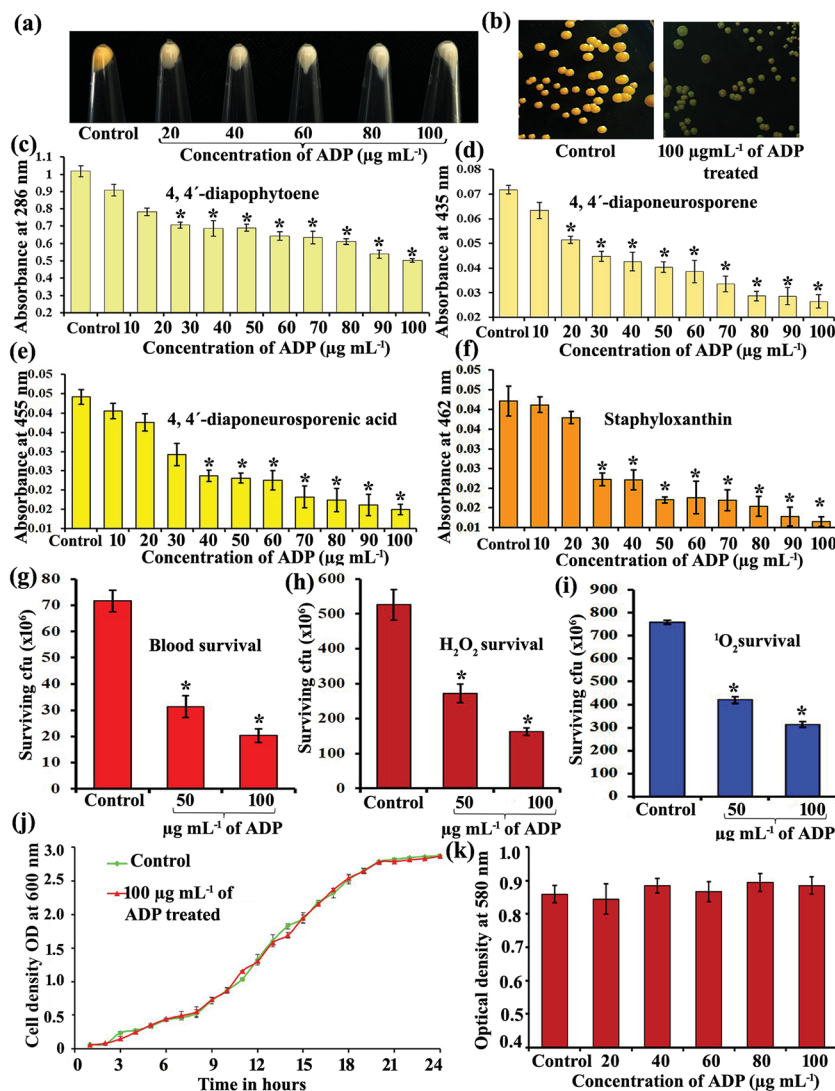


Fig. 4 Anticarotenogenic potential of ADP against MRSA. Effect of ADP treatment on the staphyloxanthin production of MRSA (a & b). Spectrophotometric assessment of the effect of ADP on 4,4'-diapophytoene (c), 4,4'-diaponeurosporene (d), 4,4'-diaponeurosporenic acid (e) and staphyloxanthin (f) production of MRSA. ADP treatment affects the ability of MRSA to survive in the presence of whole blood (g),  $\text{H}_2\text{O}_2$  (h) and methylene blue generated  $^1\text{O}_2$  (i). Effect of ADP on the growth (j) and metabolic activity (k) of MRSA. Error bars indicate SDs from the mean ( $n = 6$  (biological triplicates in technical duplicates)). Asterisks indicate a statistically significant difference ( $p < 0.05$ ).

worms (Fig. 5a). Anti-QS/antibiofilm agents have been documented for their ability to enhance the antimicrobial potential of antibiotics.<sup>57</sup> For instance, hamamelitannin has been reported to increase the activity of antibiotics against MRSA.<sup>58</sup> Furthermore, certain bioactive compounds have very meagre/no antimicrobial activity against bacterial pathogens but enhance the activity of antibiotics and are active in blocking resistance when they are administered along with antibiotics.<sup>59</sup> Such compounds are called Class I adjuvants (beta-lactamase inhibitors, efflux inhibitors, biofilm inhibitors and compounds enhancing the membrane permeability) and Class II adjuvants (compounds that enhance the antimicrobial activity by interacting with/activating the host immune response), and are collectively known as antibiotic adjuvants.<sup>59</sup> The sub-MICs of oxacillin (OXI), linezolid (LNZ), vancomycin (VAN) and rifampicin (RIF) were determined to be 128, 0.75, 0.125 and 0.01  $\mu\text{g mL}^{-1}$ , respectively. ADP was

found to be inactive in terms of antibacterial activity against MRSA even at 15  $\text{mg mL}^{-1}$ . Subsequently, the growth of MRSA in the presence of 100  $\mu\text{g mL}^{-1}$  of ADP and a sub-MIC concentration of the selected antibiotics alone or in combination was measured spectrometrically. The results revealed that combinations of antibiotics with ADP were found to be more active in inhibiting the growth of MRSA than the sub-MICs of the antibiotics alone (Fig. 5b). Recently, Trizna *et al.* have reported that treatment with furanones F35 and F83 effectively increased the susceptibility of *S. aureus* to chloramphenicol by attenuating biofilm formation, while chloramphenicol alone was inactive.<sup>60</sup> Hence, the enhanced antibacterial activity of OXI, LNZ, VAN and RIF at their sub-MICs in the presence of ADP could be attributed to the inhibition of the production of a biofilm, staphyloxanthin, slime and other virulence factors, and not to synergistic or additive activity.





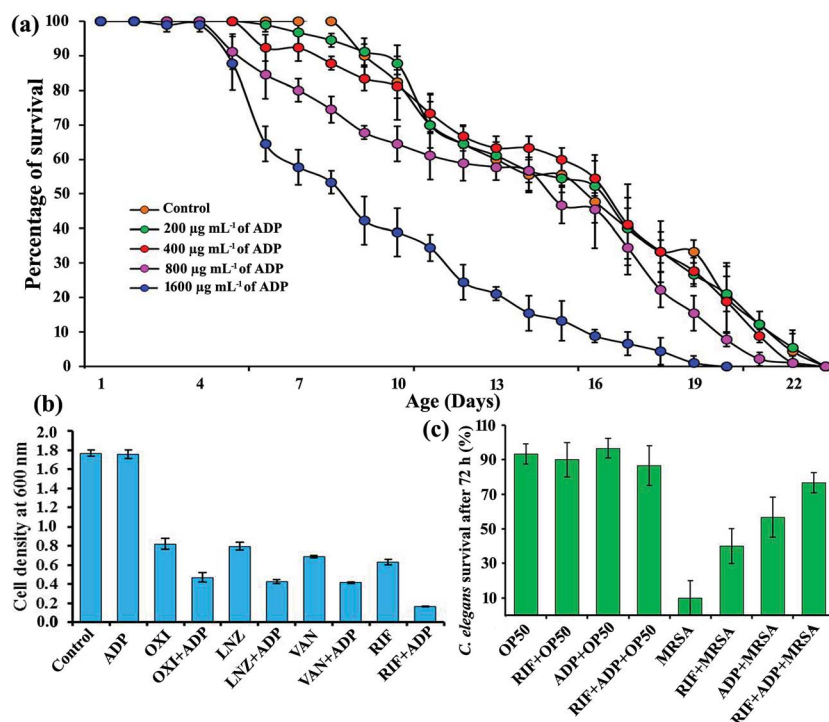


Fig. 5 Non-toxic and antibiotic adjuvant nature of ADP. Effect of higher concentrations of ADP on the survival and life span of *C. elegans* N2 (a). Effect of 100  $\mu\text{g mL}^{-1}$  of ADP, sub-MICs of antibiotics (oxiccillin (OXI), linezolid (LNZ), vancomycin (VAN) and rifampicin (RIF)) alone and in combination on the growth of MRSA (b). Effect of 100  $\mu\text{g mL}^{-1}$  of ADP, sub-MIC concentration of RIF alone and in combination on the survival of *C. elegans* N2 during MRSA infection (c). Error bars indicate SDs from the mean ( $n = 6$  (biological triplicates in technical duplicates)).

In addition, the efficacy of 100  $\mu\text{g mL}^{-1}$  of ADP, a sub-MIC concentration (0.01  $\mu\text{g mL}^{-1}$ ) of RIF and their combination on the survival of *C. elegans* during MRSA infection was analysed. The combination of antibiotics with ADP was found to be active in rescuing *C. elegans* from MRSA infection (Fig. 5c). These results further confirm the ability of ADP to enhance the activity of antibiotics in controlling the growth of MRSA. Hence, ADP can be used along with antibiotics to overcome infections caused by MRSA.

### 3.3. Effect of ADP on the expression of virulence and biofilm genes in MRSA

The accessory gene regulator (*agr*) system is known to induce the expression of toxins and extracellular virulence factors through RNA III dependent and independent pathways.<sup>61,62</sup> To study the effect of ADP on the *agr* system, the expression of the response regulator *agrA* and the transmembrane protein *agrC* was analysed. The results revealed the down-regulation of *agrC* upon ADP treatment, whereas the expression of *agrA* remained unaltered (Fig. 6). Down-regulation of *agrC* is expected to have a negative impact on the activation of virulence genes.

Interestingly, the expression of *sigB* was found to be up-regulated upon ADP treatment. *SigB* is a general stress response regulator known to regulate several cellular processes.<sup>63</sup> Mutation in *sigB* has been reported to induce the expression of virulence genes such as *sea* and *seb* (enterotoxin A & B), *aur* (aureolysin), *spc* (staphylokinase), *geh* (lipase), *hla* (alpha-

hemolysin) and *hlyB* (beta-hemolysin), and hence *sigB* has been shown to be a negative regulator of most exoenzymes and toxins.<sup>64</sup> Furthermore, *sigB* also promotes the survival of MRSA in the presence of blood,  $\text{H}_2\text{O}_2$  and UV by increasing the production of staphyloxanthin pigment.<sup>65</sup> Hence, down-regulation of virulence genes such as *geh* and *sea* upon ADP treatment could be attributed to the upregulation of *sigB*, which is known to be involved in disease progression.<sup>66</sup> These results suggest that ADP can interfere with the activation of virulence genes by modulating the expression of *sigB*.

The intracellular adhesion locus (*icaABCD*) has been shown to regulate cell-to-cell adhesion by controlling the synthesis of polysaccharides (PIA).<sup>67</sup> Gene expression analysis revealed that ADP treatment does not have any negative impact on the expression of *icaA* (*N*-acetyl glucosamine), whereas the expression of the *icaD* gene (encoding poly-beta-1,6-*N*-acetyl glucosamine biosynthesis protein) was down-regulated (Fig. 6). It has been previously reported that *icaA* requires the action of *icaD* for optimal production of PIA.<sup>68</sup> Hence down-regulation of *icaA* by ADP could be one of the mechanisms involved in the reduced biofilm formation of MRSA. *SarA* mutants have been reported to be defective in biofilm formation. In addition, compounds targeting the expression of *sarA* have been shown to have potent antibiofilm and antivirulence activity.<sup>69</sup> In contrast, ADP treatment enhanced the expression of *sarA* and *sarA*-controlled adhesion proteins *fmbA* and *fmbB* (fibronectin binding proteins). A similar expression pattern was observed in a previous study, wherein magnolol treatment induced the expression of *sarA* in

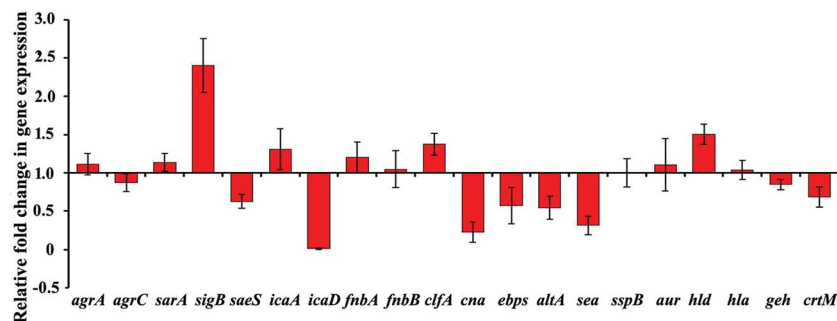


Fig. 6 Effect of ADP treatment on the gene expression of MRSA. ADP treatment modulated the expression of genes involved in *agr* signalling, biofilm formation and virulence factor production in MRSA. Error bars indicate SDs from the mean ( $n = 6$  (biological triplicates in technical duplicates)).

*S. aureus*. In addition, the dose-dependent autolysin inhibition by ADP observed in the present study agrees well with the autolysin inhibitory activity of magnolol as previously reported.<sup>70</sup> Real time PCR analysis of *altA* (autolysin) further confirms the autolysin inhibitory potential of ADP. In addition, the expression of *cna* (collagen binding protein), *saes* (histidine protein kinase), *ebps* (elastin binding protein) and *clfA* (clumping factor) was down-regulated upon ADP treatment (Fig. 6). Down-regulation of these genes involved in biofilm formation by ADP could be one of the mechanisms responsible for its antibiofilm activity.

Since *crtM* is an important enzyme involved in the biosynthesis of staphyloxanthin,<sup>18</sup> down-regulation of *crtM* by ADP could be a possible mechanism responsible for staphyloxanthin inhibition. In addition, ADP does not alter the expression of proteases such as *sspB* (cysteine protease) or *aur* (Fig. 6), which are known to be involved in biofilm disruption. In contrast to the hemolysin assay, real-time PCR analysis showed the up-regulation of *hld*, whereas the expression of *hla* remained unaltered upon ADP treatment (Fig. 6d). Owing to the detergent like structure of ADP and the results observed in the gene expression analysis, we presume that the antibiofilm activity of ADP could be multifaceted.

### 3.4. Effect of ADP on triacylglyceride accumulation, physiology and gene expression in *C. elegans*

Dehydrosqualene synthase (*CrtM*), a key enzyme involved in the initial steps of staphyloxanthin biosynthesis in MRSA, and human squalene synthase (*SQS*), involved in cholesterol biosynthesis in humans, were found to have similarity in their structures. The cholesterol biosynthesis inhibitor BPH-652 has been reported to have potent inhibitory activity against staphyloxanthin production.<sup>23</sup> In the present study, ADP inhibited staphyloxanthin production in MRSA. Hence, the effect of ADP on triglyceride accumulation was analysed using the nematode model *C. elegans*. Numerous studies have shown *C. elegans* to be one of the simplest models for studying fat metabolism and screening anti-obesity agents.<sup>26</sup> In *C. elegans*, excess energy is stored as triglycerides in the form of lipid droplets. *C. elegans* raised in high fat (25  $\mu\text{M}$  cholesterol)-containing NGM was found to exhibit increased triglyceride levels. Anti-obesity

agents such as taurine,<sup>26</sup> conjugated linoleic acid mixture,<sup>71</sup> Xenical® and Reductil®<sup>72</sup> have been found to reduce triglyceride accumulation in *C. elegans*. Furthermore, natural products such as hesperidin<sup>43</sup> and Pu-Erh tea<sup>73</sup> have been reported to mitigate triglyceride accumulation in *C. elegans*. To ascertain the effect of ADP treatment on triglyceride accumulation, *C. elegans* was raised with a high-fat diet (NGM containing 25  $\mu\text{M}$  cholesterol), and the triglyceride content was measured. The results suggested that ADP treatment reduced triglyceride accumulation in *C. elegans*. Briefly, feeding with a high-fat diet resulted in accumulation of  $\sim 74$  ng of triglyceride per worm; in contrast *C. elegans* fed a high fat diet containing 200  $\mu\text{g mL}^{-1}$  of ADP exhibited reduced triglyceride accumulation ( $\sim 51$  ng per worm) (Fig. 7a). In other words, the triglyceride content of ADP-treated *C. elegans* was found to be similar to that of *C. elegans* raised in normal NGM. In addition, the ability of ADP to inhibit triglyceride accumulation was further confirmed using Oil Red O and Sudan Black staining. Microscopic observation of worms stained with Oil Red O (Fig. 7c) and Sudan Black (Fig. 7d) showed a typical red and black coloured fat mass, respectively, in *C. elegans*. Comparison of the control, high fat diet-fed and ADP-treated *C. elegans* revealed the reduction of fat mass upon ADP treatment.

FTIR has been used as a powerful tool to study biomolecular complexes.<sup>74</sup> In the present study, FTIR was used to further authenticate the effect of ADP treatment on the triacylglyceride accumulation in *C. elegans*. The results of the FTIR analysis showed prominent signature peaks at 3000–2800  $\text{cm}^{-1}$  corresponding to fatty acids<sup>75</sup> for *C. elegans* raised in high fat diet-containing NGM. Interestingly, peaks corresponding to fatty acids were not observed in *C. elegans* raised in standard NGM or NGM supplemented with a high fat diet and 200  $\mu\text{g mL}^{-1}$  of ADP (Fig. 7e). The FTIR data undisputedly confirmed the ability of ADP to inhibit the accumulation/synthesis of triglycerides in *C. elegans*.

Pharyngeal pumping is considered to be a direct measure of active food consumption and neuronal signalling.<sup>76</sup> Hence, the effect of ADP treatment on pharyngeal pumping was monitored. The results did not show any significant difference in the pharyngeal pumping of *C. elegans* raised with a normal diet, a high fat diet and a high fat diet supplemented with 100 or 200  $\mu\text{g mL}^{-1}$  of ADP (Fig. 8a). Dietary restriction has previously been



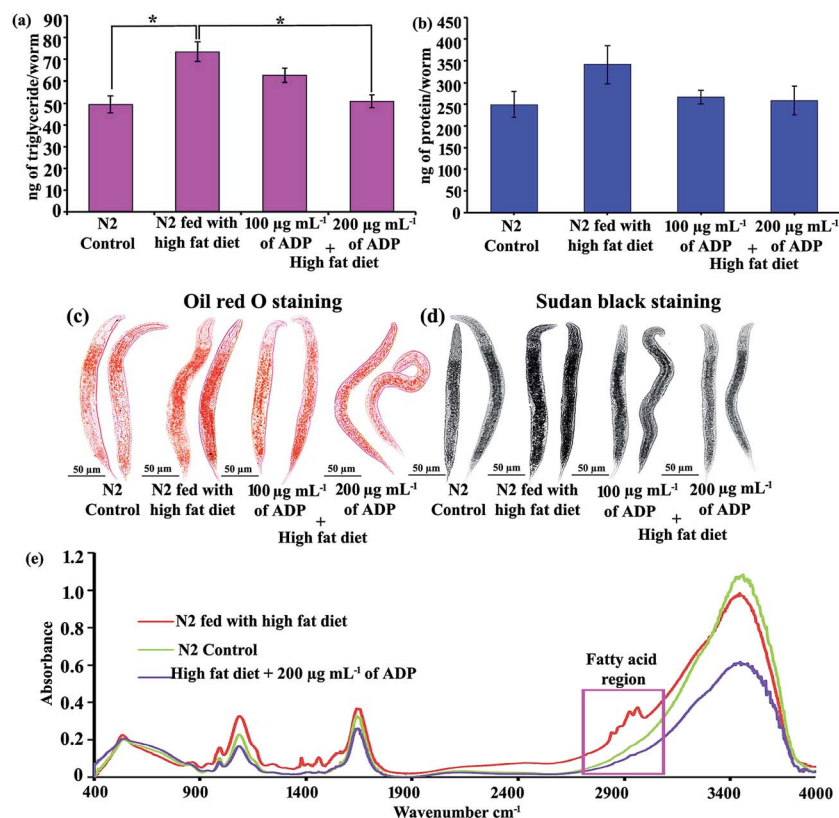


Fig. 7 Anti-obesity potential of ADP. ADP treatment reduces triacylglyceride accumulation (a) in *C. elegans* raised with a high fat diet (NGM containing 25 µM cholesterol). Effect of ADP treatment on the protein content of *C. elegans* (b). Representative light micrograph of Oil Red O (c) and Sudan Black (d) stained *C. elegans* raised with a standard diet, a high fat diet and a high fat diet supplemented with ADP (400× magnification). Fourier transform infrared (FTIR) analysis of control, high fat diet and ADP-treated whole worms (e). Error bars indicate SDs from the mean ( $n = 6$  (biological triplicates in technical duplicates)). Asterisks indicate a statistically significant difference ( $p < 0.05$ ).

reported to reduce the fat accumulation, brood size and longevity of *C. elegans*.<sup>77,78</sup> Hence we analysed the influence of ADP treatment on food consumption using a 24-well MTP plate assay by incubating *C. elegans* ( $N = 50$ ) raised in standard NGM, and high fat-containing NGM without and with 100 or 200 µg mL<sup>-1</sup> of ADP in M9 buffer containing heat UV irradiated *E. coli* OP50 ( $OD_{600} = 0.4$ ) as a food source, and there was no significant difference in the reduction in cell density (Fig. 8b). These results indicate that ADP did not have any negative impact on food consumption in *C. elegans*.

In addition, the effect of ADP on the brood size of *C. elegans* was also analysed and the results revealed that there was no significant difference in progeny production during the observed period (Fig. 8c). Furthermore, the effect of ADP on the locomotion of *C. elegans* was assessed by measuring the body bend count per minute. There was no significant difference in the mean body bend count of *C. elegans* ( $N = 10$ ) raised in standard NGM, and high fat-containing NGM without and with 100 or 200 µg mL<sup>-1</sup> of ADP (Fig. 8d). The results of the locomotion assay suggested that ADP did not have any modulatory effect on the cholinergic system of *C. elegans*. Interestingly, fluorescence microscopic analysis of 2',7'-dichlorodihydrofluorescein diacetate (H<sub>2</sub>DCFDA)-stained worms revealed a reduction in reactive oxygen species (ROS) generation in ADP-

treated *C. elegans* as compared to high fat diet-fed *C. elegans* (Fig. 8e). Inhibition of ROS generation suggested that ADP does not exert any oxidative stress on *C. elegans*.

In *C. elegans*,  $\Delta 9$  desaturases/stearoyl-CoA desaturases such as fat-5, fat-6 and fat-7 are involved in the synthesis of oleic acid by converting palmitic acid to palmitoleic acid, and palmitoleic acid to stearic acid, followed by the conversion of stearic acid to oleic acid, respectively.<sup>79</sup> Loss of fat-6 leads to a reduction in long chain unsaturated fatty acids in *C. elegans*.<sup>80</sup> Interestingly, ADP down-regulated the expression of fat-6 even in the presence of cholesterol (Fig. 8e). Since, oleic acid is a primary substrate for the biosynthesis of triglycerides and other complex lipids, down-regulation of fat-6 by ADP could be a possible mode of action responsible for the quelling of triacylglyceride accumulation in *C. elegans*. Fatty acid metabolism in *C. elegans* is also regulated by DAF-2/insulin like signalling (ILS),<sup>81</sup> and hence in the present study we have analysed the effect of ADP treatment on genes involved in the DAF-2/ILS pathway, such as *ins-7* (insulin/IGF-1-like peptide), *daf-2* (insulin/IGF receptor ortholog), *daf-16* (forkhead box O (FOXO) homologue), *age-1* (phosphoinositide 3-kinase), *akt-1* (serine/threonine kinase), *sgk-1* (serine/threonine protein kinase) and *skn-1* (bZip transcription factor ortholog). The expression of *daf-16* was upregulated and *ins-7*, *age-1* and *sgk-1* are found to be down-regulated upon ADP treatment (Fig. 8f). It





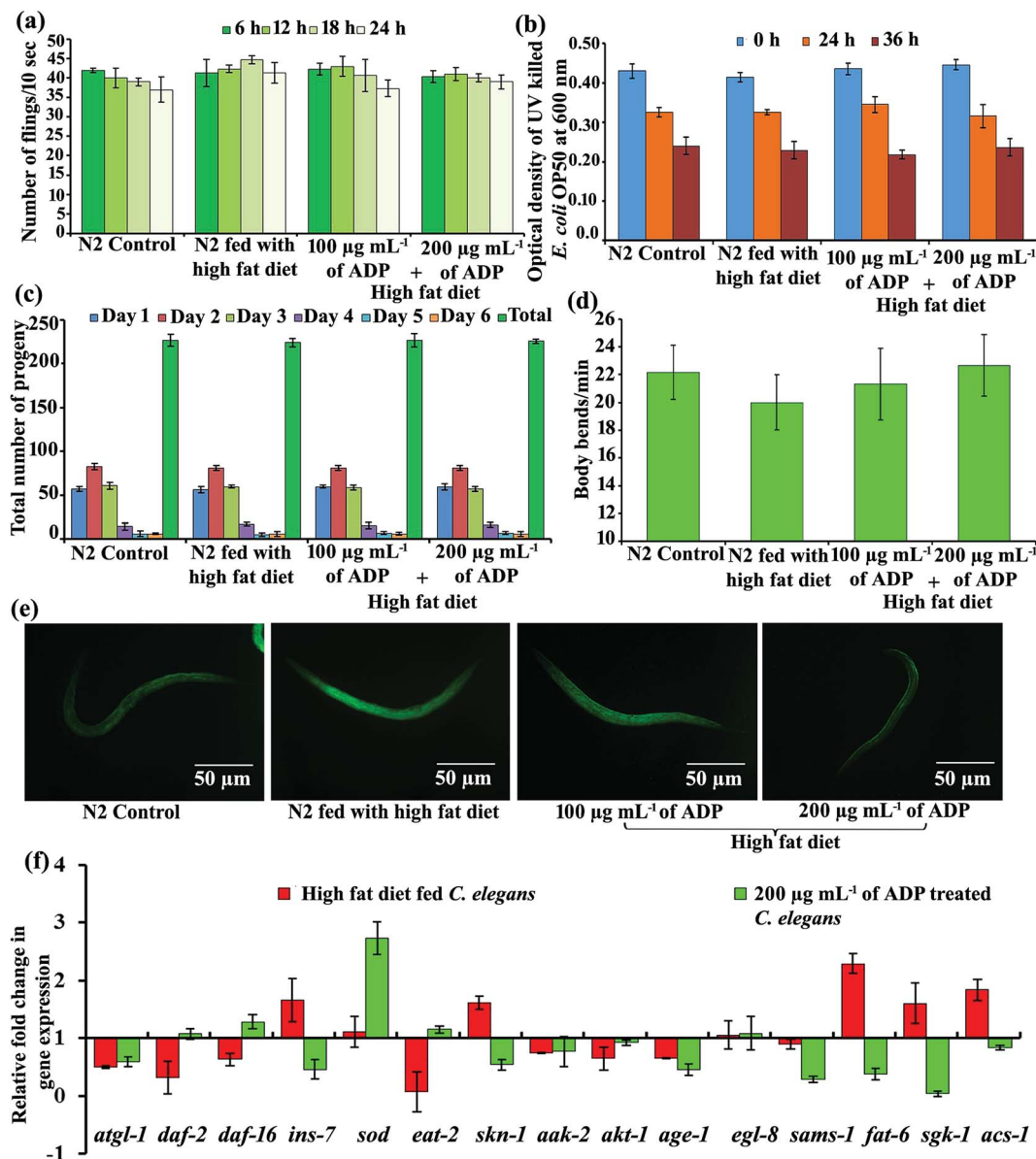


**Fig. 8** Effect of ADP on physiology, reproduction, ROS generation and gene expression of *C. elegans*. ADP treatment does not alter pharyngeal pumping (a), food consumption (b), brood size (c) or thrashing (d). Representative fluorescence micrograph of H<sub>2</sub>DCFDA-stained high fat diet-fed and ADP-treated *C. elegans* showing the increased and decreased accumulation of ROS (e). Differential expression of genes involved in fatty acid synthesis, insulin signalling, food uptake, reproduction and oxidative stress. Error bars indicate SDs from the mean ( $n = 6$  (biological triplicates in technical duplicates)).

has been previously reported that the binding of *ins-7* to *daf-2* is necessary for the expression of *age-1* and *pdk-1* and the phosphorylation of *akt-1/2* and *sgk-1*, which in turn phosphorylates *daf-16*. Phosphorylation of *daf-16* blocks its nuclear translocation and reduces the lifespan of *C. elegans*.<sup>82</sup> Upregulation of *daf-16* and down-regulation of *ins-7* by ADP could be a possible mechanism responsible for the normal lifespan of *C. elegans*. Similar to *daf-2* mutants, *age-1* mutants have also been reported to exhibit an extended lifespan.<sup>83</sup> Down-regulation of *age-1* and upregulation of *sod* (superoxide dismutase) by ADP (Fig. 8f) agrees well with a previous study, wherein *age-1* mutants produced an increased level of antioxidant enzymes such as

superoxide dismutase and catalase when compared to the parental strain.<sup>84</sup> Furthermore, *sgk-1*-mediated Rictor/TORC2 regulation is responsible for fat storage and development of *C. elegans* and the loss of *sgk-1* leads to a reduction in fat storage and an increase in the level of reactive oxygen species (ROS).<sup>85</sup> Upregulation of *sod* by ADP could be the key mechanism responsible for the reduction of ROS accumulation in *C. elegans* as evidenced by fluorescence microscopy analysis using DCFDA.

Furthermore, ADP treatment also down-regulated *S*-adenosylmethionine synthase (*sams-1*), which is a known methyl group donor in many biochemical reactions (Fig. 8f). Knock-down of *sams-1* has been reported to increase the lifespan of



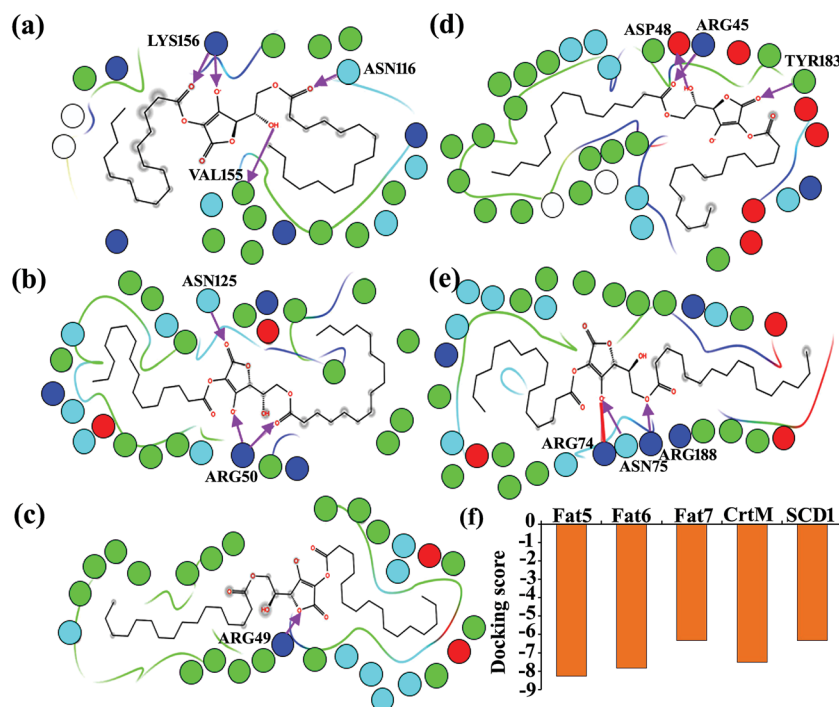


Fig. 9 Molecular docking. Representative images depicting the predicted interactions of ADP with proteins involved in oleic acid synthesis [ $\Delta 9$  desaturases fat-5, fat-6 and fat-7] in *C. elegans* (a, b & c), staphyloxanthin synthesis (dehydroxysqualene synthase CrtM) in MRSA (d) and fatty acid metabolism (SCD1) in humans (e). Graphical representation of the docking scores (f).

wild-type *C. elegans*.<sup>86</sup> Metformin, a biguanide drug, is used as an oral drug to control type 2 diabetes and its supplementation in NGM was found to cause dietary restriction by down regulating the expression of *sams-1*.<sup>87</sup> In contrast, ADP did not cause any effect similar to dietary restriction in *C. elegans* as evidenced by the food consumption and pharyngeal pumping assay. Furthermore, the expression of *eat-2* (ligand-gated ion channel subunit) was found to be normal upon ADP treatment (Fig. 8f) and hence the reduction of fat accumulation could be due to inhibition of fatty acid biosynthesis and not dietary restriction. *C. elegans* depends on *atgl-1* (adipose triglyceride lipase 1) for the generation of free fatty acids from stored fat droplets and maintains lipid homeostasis.<sup>88</sup> The insignificant difference in the expression of *atgl-1* in *C. elegans* raised with a high fat diet and a high fat diet supplemented with ADP indicated that the reduction in triglyceride accumulation is due to ADP treatment and not due to the expression of *atgl-1*. In addition, ADP does not have any impact on the expression of *egl-8*, responsible for egg laying (Fig. 8f).

### 3.5. Molecular docking analysis

Structure-based virtual screening methods have successfully been employed for the identification and design of a wide range of pharmacologically active compounds against drug targets. In addition, *in silico* approaches are also used to predict the interaction of known druggable target proteins and their native ligands/drugs.<sup>27,45</sup> The precursor molecules of staphyloxanthin biosynthesis and triglyceride biosynthesis in *C. elegans*, such as

2× farnesyl diphosphate<sup>23</sup> and palmitoleic acid,<sup>79</sup> respectively, share structural similarity with ADP and hence ADP could act as a competitive inhibitor. Hence, in the present study, ADP was docked with CrtM (involved in the first step of staphyloxanthin biosynthesis of MRSA) and fat-5, fat-6 and fat-7 (involved in the oleic acid biosynthesis of *C. elegans*) to probe their interaction. Furthermore, human stearoyl-coenzyme A desaturase-1 (SCD1) has been proven as a druggable target to design therapeutic agents to treat metabolic diseases, and hence SCD1 was also included in the molecular docking study. The results of the molecular docking studies predicted the ability of ADP to interact with all of the selected target proteins. Briefly, ADP interacts with the active sites of fat-5, fat-6 and fat-7 through 3 hydrogen bonding interactions (Val 155, Asn 116 and Lys 156) (Fig. 9a), 2 hydrogen bonding interactions (Asn 125 and Arg 50) (Fig. 9b) and one hydrogen bonding interaction (Arg 49) (Fig. 9c), respectively. In the case of CrtM, ADP interacts through 3 hydrogen bonding interactions (Arg 45, Asp 48 and Tyr 183) (Fig. 9d). ADP also interacts with human SCD1, which is involved in fatty acid metabolism, through 2 hydrogen bonding interactions (Asn 75 and Arg 188) and a salt bridge interaction (Arg 74) (Fig. 9e). These results imply that the binding of ADP to the active sites of target enzymes involved in oleic acid production could be a possible mechanism responsible for the reduction of triglyceride accumulation in *C. elegans*.

Treatment of *S. aureus* with rhodomyrtone has been reported to inhibit staphyloxanthin production by down-regulating the expression of *sigB*. However, in the present study, ADP treatment was found to upregulate *sigB* expression and we speculate



that the inhibition of staphyloxanthin production could be due to a *sigB*-independent mechanism. Based on the molecular docking analysis and the structural similarity of  $2\times$  farnesyl diphosphate with ADP, it is hypothesized that the interaction of ADP with CrtM, as well as down-regulation of *crtM*, could be a plausible mechanism responsible for staphyloxanthin biosynthesis in MRSA.

## 4. Conclusion

The current study reveals that ADP has antibiofilm, anti-pathogenic and anticarotenogenic potential. ADP inhibited biofilm, lipase, hemolysin, and protease production in a concentration-dependent manner. qPCR analysis revealed the differential expression of genes involved in biofilm formation and virulence factor production in MRSA upon ADP treatment. In addition, ADP profoundly inhibited the carotenoid pigment staphyloxanthin, and hence its effect on triacylglyceride accumulation in *C. elegans* was also assessed. Interestingly, ADP was found to reduce triacylglyceride accumulation in *C. elegans* without exerting any negative impact on lifespan, food consumption, brood size *etc.* Microscopic observation of Oil Red and Sudan Black stained *C. elegans* raised with a normal diet, high fat diet and high fat diet supplemented with ADP showed the reduction of triacylglyceride accumulation. qPCR analysis revealed the differential expression of genes involved in fatty acid synthesis, insulin signalling and stress response. Furthermore, molecular docking analysis predicted the ability of ADP to bind with the active sites of CrtM in MRSA, and fat-5, fat-6 and fat-7 in *C. elegans* involved in staphyloxanthin and oleic acid biosynthesis, respectively. Owing to its non-toxic nature, antibiofilm and antivirulence potential against MRSA, and triacylglyceride inhibitory activity in *C. elegans*, ADP holds promise for application in the field of medical microbiology and metabolic syndrome therapeutics.

## Conflicts of interests

The authors declare no competing financial interests.

## Acknowledgements

The authors are grateful for the computational facility provided by the Bioinformatics Infrastructure Facility funded by the Department of Biotechnology, Government of India [grant number BT/BI/25/015/2012(BIF)]. The Instrumentation Facility provided by Department of Science and Technology, Government of India through PURSE [grant number SR/S9Z-3/2010/42(G)] and FIST [grant number SR-FST/LSI-087/2008], and the University Grants Commission (UGC), New Delhi through SAP-DRS1 [grant number F.3-28/2011 (SAP-II)] are gratefully acknowledged. The authors are also grateful to Caenorhabditis Genetics Center for providing *C. elegans* N2 WT and *E. coli* OP50. S. S. and A. V. acknowledge the fellowship provided by DBT through BIF, and L. V. acknowledges the Basic Scientific Research Fellowship provided by UGC [grant number F.4-1/2006(BSR)/7-326/2011(BSR)].

## References

- 1 S. Veerachamy, T. Yarlagadda, G. Manivasagam and P. K. Yarlagadda, *Proc. Inst. Mech. Eng., Part H*, 2014, **228**, 1083.
- 2 C. Potera, *Science*, 1999, **283**, 1837.
- 3 NIH RESEARCH ON MICROBIAL BIOFILMS. Available online: <http://grants.nih.gov/grants/guide/pa-files/PA-03-047.html>.
- 4 H. C. Flemming, T. R. Neu and D. J. Wozniak, *J. Bacteriol.*, 2007, **189**, 7945.
- 5 T. F. Mah and G. A. O'Toole, *Trends Microbiol.*, 2001, **9**, 34.
- 6 N. Hoiby, T. Bjarnsholt, M. Givskov, S. Molin and O. Ciofu, *Int. J. Antimicrob. Agents*, 2010, **35**, 322.
- 7 P. S. Stewart and J. W. Costerton, *Lancet*, 2001, **358**, 135.
- 8 H. Van Acker, P. Van Dijk and T. Coenye, *Trends Microbiol.*, 2014, **22**, 326.
- 9 H. F. Wertheim, D. C. Melles, M. C. Vos, W. van Leeuwen, A. van Belkum, H. A. Verbrugh and J. L. Nouwen, *Lancet Infect. Dis.*, 2005, **5**, 751.
- 10 T. S. Naimi, K. H. LeDell, K. Como-Sabetti, S. M. Borchardt, D. J. Boxrud, J. Etienne, S. K. Johnson, F. Vandenesch, S. Fridkin, C. O'boyle and R. N. Danila, *Jama.*, 2003, **290**, 2976.
- 11 B. Tarai, P. Das and D. Kumar, *J. Lab. Physicians*, 2013, **5**, 71.
- 12 S. Y. Tong, J. S. Davis, E. Eichenberger, T. L. Holland and V. G. Fowler, *Clin. Microbiol. Rev.*, 2015, **28**, 603.
- 13 J. L. Lister and A. R. Horswill, *Front. Cell. Infect. Microbiol.*, 2015, **5**, 31.
- 14 L. G. Harris and R. G. Richards, *Injury*, 2006, **37**, S3.
- 15 C. P. Gordon, P. Williams and W. C. Chan, *J. Med. Chem.*, 2013, **56**, 1389.
- 16 M. M. Dinges, P. M. Orwin and P. M. Schlievert, Exotoxins of *Staphylococcus aureus*, *Clin. Microbiol. Rev.*, 2000, **13**, 16–34.
- 17 A. Clauditz, A. Resch, K. P. Wieland, A. Peschel and F. Götz, *Infect. Immun.*, 2006, **74**, 4950.
- 18 A. Pelz, K. P. Wieland, K. Putzbach, P. Hentschel, K. Albert and F. Götz, *J. Biol. Chem.*, 2005, **280**, 32493.
- 19 S. Sethupathy, A. Valliammai, B. Shanmuganathan and S. K. Pandian, *Recent trends in biosciences.*, 2016, vol. 79, p. OMM-06.
- 20 M. H. Lien, B. C. Huang and M. C. Hsu, *J. Chromatogr. A*, 1993, **645**, 362.
- 21 A. R. Elmore, *Int. J. Toxicol.*, 2004, **24**, 51.
- 22 S. Fukushima, T. Ogiso, Y. Kurata, M. A. Shibata and T. Kakizoe, *Cancer Lett.*, 1987, **35**, 17.
- 23 C. I. Liu, G. Y. Liu, Y. Song, F. Yin, M. E. Hensler, W. Y. Jeng, V. Nizet, A. H. Wang and E. Oldfield, *Science*, 2008, **319**, 1391.
- 24 R. M. McKay, J. P. McKay, L. Avery and J. M. Graff, *Dev. Cell*, 2003, **4**, 131.
- 25 Y. Zhang, X. Zou, Y. Ding, H. Wang, X. Wu and B. Liang, *BMC Genomics*, 2013, **14**, 1.
- 26 H. M. Kim, C. H. Do and D. H. Lee, *J. Biomed. Sci.*, 2010, **17**, 1.
- 27 S. Sethupathy, C. Nithya and S. K. Pandian, *Biofouling*, 2015, **31**, 721.
- 28 M. Sandasi, C. M. Leonard and A. M. Viljoen, *Lett. Appl. Microbiol.*, 2010, **50**, 30.





- 29 J. N. Walker and A. R. Horswill, *Front. Cell. Infect. Microbiol.*, 2012, **2**, 162.
- 30 S. Gowrishankar, N. M. Duncun and S. K. Pandian, *J. Evidence-Based Complementary Altern. Med.*, 2012, 862374.
- 31 F. G. Sorroche, M. B. Spesia, Á. Zorreguieta and W. Giordano, *Appl. Environ. Microbiol.*, 2012, **78**, 4092.
- 32 D. J. Freeman, F. R. Falkiner and C. T. Keane, *J. Clin. Pathol.*, 1989, **42**, 872.
- 33 A. Annapoorani, R. Parameswari, S. K. Pandian and A. V. Ravi, *J. Microbiol. Methods*, 2012, **91**, 208.
- 34 K. Riedel, D. Talker-Huiber, M. Givskov, H. Schwab and L. Eberl, *Appl. Environ. Microbiol.*, 2003, **69**, 3901.
- 35 N. A. Mani, P. H. Tobin and R. K. Jayaswal, *J. Bacteriol.*, 1993, **175**.
- 36 G. Y. Liu, A. Essex, J. T. Buchanan, V. Datta, H. M. Hoffman, J. F. Bastian, J. Fierer and V. Nizet, *J. Exp. Med.*, 2005, **202**, 209.
- 37 S. Brenner, *Genetics*, 1974, **77**, 71.
- 38 L. Gao, R. Zhang, J. Lan, R. Ning, D. Wu, D. Chen and W. Zhao, *J. Nat. Prod.*, 2016, **79**, 3039.
- 39 K. Yen, T. T. Le, A. Bansal, S. D. Narasimhan, J. X. Cheng and H. A. Tissenbaum, *PLoS One*, 2010, **5**, e12810.
- 40 B. Vigneshkumar, S. K. Pandian and K. Balamurugan, *Arch. Microbiol.*, 2012, **194**, 229.
- 41 P. Kesika, S. K. Pandian and K. Balamurugan, *Scand. J. Infect. Dis.*, 2011, **43**, 286.
- 42 D. Gems and D. L. Riddle, *Genetics*, 2000, **154**, 1597.
- 43 H. Peng, Z. Wei, H. Luo, Y. Yang, Z. Wu, L. Gan and X. Yang, *J. Agric. Food Chem.*, 2016, **64**, 5207.
- 44 S. Durai, N. Singh, S. Kundu and K. Balamurugan, *Proteomics*, 2014, **14**, 1820.
- 45 A. K. Kahlon, S. Roy and A. Sharma, *J. Biomol. Struct. Dyn.*, 2010, **28**, 201.
- 46 Z. Song, L. Borgwardt, N. Høiby, H. Wu, T. S. Sørensen and A. Borgwardt, *Orthop. Res. Rev.*, 2013, **5**, e14.
- 47 H. S. Cho, J. H. Lee, M. H. Cho and J. Lee, *Biofouling*, 2015, **31**, 1.
- 48 P. Houston, S. E. Rowe, C. Pozzi, E. M. Waters and J. P. O'Gara, *Infect. Immun.*, 2011, **79**, 1153.
- 49 G. J. Lyon and R. P. Novick, *Peptides*, 2004, **25**, 1389.
- 50 M. Chu, M. B. Zhang, Y. C. Liu, J. R. Kang, Z. Y. Chu, K. L. Yin, L. Y. Ding, R. Ding, R. X. Xiao, Y. N. Yin and X. Y. Liu, *Sci. Rep.*, 2016, **6**, 24748.
- 51 J. H. Lee, Y. G. Kim, K. Lee, C. J. Kim, D. J. Park, Y. Ju, J. C. Lee, T. K. Wood and J. Lee, *Biofouling*, 2016, **32**, 45.
- 52 K. Yamashita, *Proc. Natl. Acad. Sci. U. S. A.*, 2011, **108**, 17314.
- 53 C. P. Gordon, P. Williams and W. C. Chan, *J. Med. Chem.*, 2013, **56**, 1389.
- 54 C. I. Liu, W. Y. Jeng, W. J. Chang, T. P. Ko and A. H. Wang, *J. Biol. Chem.*, 2012, **287**, 18750.
- 55 S. Leejae, L. Hasap and S. P. Voravuthikunchai, *J. Med. Microbiol.*, 2013, **62**, 421.
- 56 T. B. Rasmussen and M. Givskov, *Microbiol.*, 2006, **152**, 895.
- 57 G. Brackman, P. Cos, L. Maes, H. J. Nelis and T. Coenye, *Antimicrob. Agents Chemother.*, 2011, **55**, 2655.
- 58 G. Brackman, K. Breyne, R. De Rycke, A. Vermote, F. Van Nieuwerburgh, E. Meyer, S. Van Calenbergh and T. Coenye, *Sci. Rep.*, 2016, **6**, 20321.
- 59 G. D. Wright, *Trends Microbiol.*, 2016, **24**, 862.
- 60 E. Y. Trizna, E. N. Khakimullina, L. Z. Latypova, A. R. Kurbangalieva, I. S. Sharafutdinov, V. G. Evtugin, E. V. Babynin, M. I. Bogachev and A. R. Kayumov, *Acta Naturae.*, 2015, **7**, 102.
- 61 S. Y. Queck, M. Jameson-Lee, A. E. Villaruz, T. H. Bach, B. A. Khan, D. E. Sturdevant, S. M. Ricklefs, M. Li and M. Otto, *Mol. Cell*, 2008, **32**, 150.
- 62 C. Kong, H. M. Neoh and S. Nathan, *Toxins*, 2016, **8**, 72.
- 63 P. C. Loewen and R. Hengge-Aronis, *Annu. Rev. Microbiol.*, 1994, **48**, 53.
- 64 M. Bischoff, P. Dunman, J. Kormanec, D. Macapagal, E. Murphy, W. Mounts, B. Berger-Bächi and S. Projan, *J. Bacteriol.*, 2004, **186**, 4085.
- 65 I. Kullik, I. Giachino and T. Fuchs, *J. Bacteriol.*, 1998, **180**, 4814.
- 66 E. Ortega, H. Abriouel, R. Lucas and A. Galvez, *Toxins*, 2010, **2**, 2117.
- 67 S. E. Cramton, C. Gerke, N. F. Schnell, W. W. Nichols and F. Gotz, *Infect. Immun.*, 1999, **67**, 5427.
- 68 D. Cue, M. G. Lei and C. Y. Lee, Genetic regulation of the intercellular adhesion locus in staphylococci, *Front. Cell. Infect. Microbiol.*, 2012, **2**, 149.
- 69 R. Arya, R. Ravikumar, R. S. Santhosh and S. Princy, *Front. Microb. Immunol.*, 2015, **6**, 416.
- 70 D. Wang, Q. Jin, H. Xiang, W. Wang, N. Guo, K. Zhang, X. Tang, R. Meng, H. Feng, L. Liu and X. Wang, *PloS one*, 2011, **6**, e26833.
- 71 P. Martorell, S. Llopis, N. González, F. Montón, P. Ortiz, S. Genovés and D. Ramón, *J. Agric. Food Chem.*, 2012, **60**, 11071.
- 72 L. Aitlhadj and S. R. Stürzenbaum, *Toxicol. Res.*, 2013, **2**, 145.
- 73 Y. Ding, X. Zou, X. Jiang, J. Wu, Y. Zhang, D. Chen and B. Liang, *PloS one*, 2015, **10**, e0113815.
- 74 B. H. Stuart, Infrared spectroscopy of biological applications, *Encyclopaedia of Analytical Chemistry*, John Wiley & Sons Ltd., Chichester, 2000, p. 529.
- 75 D. Helm, H. Labischinski, G. Schallehn and D. Naumann, *J. Gen. Microbiol.*, 1991, **137**, 69.
- 76 B. B. Shtonda and L. Avery, *J. Exp. Biol.*, 2006, **209**, 89.
- 77 S. Emran, M. Yang, X. He, J. Zandveld and M. D. Piper, *Aging*, 2014, **6**, 390.
- 78 L. Avery and H. R. Horvitz, *J. Exp. Zool.*, 1990, **253**, 263.
- 79 J. L. Watts, *Trends Endocrinol. Metab.*, 2009, **20**, 58.
- 80 T. J. Brock, J. Browse and J. L. Watts, *Genetics*, 2012, **176**, 865.
- 81 L. R. Lapierre and M. Hansen, *Trends Endocrinol. Metab.*, 2012, **23**, 637.
- 82 C. T. Murphy, *Exp. Gerontol.*, 2006, **41**, 910.
- 83 J. B. Dorman, B. Albinder, T. Shroyer and C. Kenyon, *Genetics*, 1995, **141**, 1399.
- 84 P. L. Larsen, *Proc. Natl. Acad. Sci. U. S. A.*, 1993, **90**, 8905.
- 85 K. T. Jones, E. R. Greer, D. Pearce and K. Ashrafi, *PLoS Biol.*, 2009, **7**, e1000060.
- 86 M. Hansen, A. L. Hsu, A. Dillin and C. Kenyon, *PLoS Genet.*, 2005, **1**, 119.
- 87 F. Cabreiro, C. Au, K. Y. Leung, N. Vergara-Irigaray, H. M. Cochemé, T. Noori, D. Weinkove, E. Schuster, N. D. Greene and D. Gems, *Cell*, 2013, **153**, 228.
- 88 J. H. Lee, J. Kong, J. Y. Jang, J. S. Han, Y. Ji, J. Lee and J. B. Kim, *Mol. Cell. Biol.*, 2014, **34**, 4165.

